

See discussions, stats, and author profiles for this publication at: <https://www.researchgate.net/publication/14748546>

# Insertion of peptide chains into lipid membranes: An off-lattice Monte Carlo dynamics model

ARTICLE *in* PROTEINS STRUCTURE FUNCTION AND BIOINFORMATICS · JANUARY 1993

Impact Factor: 2.63 · DOI: 10.1002/prot.340150104 · Source: PubMed

---

CITATIONS

111

---

READS

21

## 2 AUTHORS:



**Mariusz Milik**

Selvita S.A.

34 PUBLICATIONS 692 CITATIONS

SEE PROFILE



**Jeffrey Skolnick**

Georgia Institute of Technology

381 PUBLICATIONS 16,807 CITATIONS

SEE PROFILE

# Insertion of Peptide Chains Into Lipid Membranes: An Off-Lattice Monte Carlo Dynamics Model

Mariusz Milik and Jeffrey Skolnick

*Department of Molecular Biology, The Scripps Research Institute, La Jolla, California 92037*

**ABSTRACT** A combination of dynamic Monte Carlo simulation techniques with a hydropathy scale method for the prediction of the location of transmembrane fragments in membrane proteins is described. The new hydropathy scale proposed here is based on experimental data for the interactions of tripeptides with phospholipid membranes (Jacobs, R.E., White, S.H. *Biochemistry* 26:6127–6134, 1987) and the self-solvation effect in protein systems (Roseman, M.A., *J. Mol. Biol.* 200:513–522, 1988). The simulations give good predictions both for the state of association and the orientation of the peptide relative to the membrane surface of a number of peptides including Magainin2, M26, and melittin. Furthermore, for Pf1 bacteriophage coat protein, in accord with experiment, the simulations predict that the C-terminus forms a transmembrane helix and the N-terminus forms a helix which is adsorbed on the surface of the bilayer. Finally, the present series of simulations provide a number of insights into the mechanism of insertion of peptides into cell membranes. © 1993 Wiley-Liss, Inc.

**Key words:** peptide chains, lipid membranes, Monte Carlo simulation techniques, hydropathy scale method, tripeptides, phospholipid membranes

## INTRODUCTION

The problem of insertion of peptide chains into cell membranes is of fundamental importance in the area of membrane protein research. This is reflected in the growing attention this field has received from both theory and experiment.<sup>1–11</sup> Recently, computer simulations have emerged as a powerful technique to guide the development of both theoretical and experimental methods. There are many key questions where simulations can provide a number of insights. These include the mechanism of protein insertion into bilayers, the differential interactions between amino acids in water and in lipid phases, the modification of the structure of the lipid accompanying peptide insertion, the location of transmembrane helices and extramembrane loops, and more generally, the preferred location of peptide fragments relative to the membrane. In the present paper, we consider

simplified models which are designed to address these questions and demonstrate that it is possible, at least for simple geometries, to predict the conformation of peptides and small proteins using an effective medium model of a membrane.

Use of computer simulations to probe various facets of protein/membrane systems has already provided a number of insights. For example, Edholm and Johansson<sup>12</sup> have used molecular dynamics to simulate a short, trans-bilayer fragment of glycophorin. This model contains a hundred lipid molecules forming a bilayer, and one trans-bilayer peptide in the helix conformation. Use of a full atom representation of the lipid molecules provides the possibility of exploring the effects of a trans-bilayer helix on the structural and dynamic properties of the bilayer; however, this model neglects hydrophobic interactions. As was subsequently pointed out by Edholm and Jahnig,<sup>13</sup> the hydrophobic effect is very difficult to model on an atomic level. When a full representation of the peptide, lipids, and water is employed, there is a large error because the effective lipid-protein interactions arise from the small difference between the strong interactions of the protein atoms with the atoms of water and the lipid.<sup>13</sup> Starting from analogous assumptions, Edholm and Jahnig<sup>13</sup> used a continuum approximation for the hydrophobic effect, and by employing phenomenological energies, they have modelled a 46-residue fragment of glycophorin. As before, the simulation started from an initial helical and trans-bilayer configuration. The elapsed simulation time (about 100 psec) permitted an examination of the structural fluctuations in the trans-bilayer conformation of glycophorin.

Starting from helical structures obtained from both crystallography and from NMR data, Pastore et al.<sup>14</sup> have simulated the toxin melittin using the GROMOS MD package. These simulations neglect the hydrophobic effect as well as the presence of the water and lipid molecules and simulate the system for relatively short times (20–30 psec). These simu-

Received May 26, 1992; revision accepted July 24, 1992.

Address reprint requests to Dr. Jeffrey Skolnick, Department of Molecular Biology, The Scripps Research Institute, 10666 North Torrey Pines Road, La Jolla, CA 92037.

lations represent an interesting attempt to glean some aspects of the behavior of melittin. Unfortunately, the actual experimental situation is more complicated, e.g., melittin is not monomeric in water, and longer times are required to achieve equilibrium sampling. This necessitates the development of alternative techniques such as are presented here.

Based upon our previous simulations of lipid-water systems<sup>15</sup> and a lattice model of membrane peptides,<sup>16</sup> we propose an off-lattice Monte Carlo dynamics model of peptide chains in membranes. Our model is designed to simulate the properties of short helical peptides in the membrane phase; for these preliminary calculations, we employ a simple C $\alpha$  representation of the peptide chain having helical propensities and a mean-field, effective medium representation of the membrane phase. As a necessary consequence, we cannot explore differences in secondary structural preferences for  $\alpha$ -helices or  $\beta$ -sheets of the peptides (however, turns versus  $\alpha$ -helices preferences can be examined; see for example Pfl virus coat protein) nor the changes in lipid phase structure. However, we can use phenomenological interaction parameters to obtain some important information about the orientation of helical fragments in the membrane and some information about the insertion pathway.

The development of a good set hydrophobic interaction parameters is especially crucial to the success of the method. Starting from the Jacobs and White multiphase-membrane system<sup>4</sup> and Roseman's study of the self-solvation effect,<sup>17</sup> we have built a new hydrophathy scale, which can be explicitly used in the Monte Carlo simulation. The effects of changes in the lipid chain ordering in the neighborhood of peptide chain and the coupling between peptide location (in, on, or across the bilayer) and hydrophobic interactions are also schematically addressed in the present model.

The outline of the remainder of the paper is as follows. The next section contains a description of the model including the proposed hydrophathy scale and an overview of the Monte Carlo algorithm. The results of the simulations for a set of representative peptides are then presented. Finally, the paper concludes with a discussion of the results of the simulations, their relationship to experimental data, and the advantages and disadvantages of the proposed model.

## DESCRIPTION OF MODEL

A C- $\alpha$  representation of the peptides is used, where the distance between adjacent residues equals 3.785 Å (1 Å = 0.1 nm), which is the mean value of the C $\alpha$ -C $\alpha$  distance for proteins represented in the Brookhaven Protein Database. Excluded volume is implemented as a hardcore interaction between residues. The values of the interaction radii

are taken from Table I of Gregoret and Cohen,<sup>18</sup> calculated using a "sphere growth method." While Gregoret and Cohen used two or three balls to represent the aromatic amino acids, here for simplicity, a single ball representation is used for every amino acid.

The Monte Carlo dynamics method is used to calculate the equilibrium properties of the model system. The system starts from a random conformation and then diffuses in conformational space by randomly chosen micro-modifications of the peptide chain conformation. The time interval is discrete, and at every moment  $t_i$ , the transition probability from state  $S(t_i)$  to state  $S(t_i+1)$  depends on the energy of these states, according to the asymmetrical Metropolis scheme.<sup>19</sup> The set of micromodifications is very limited and contains only "spike" moves for the central and end segments, and a "sliding" move. The "spike" move (illustrated in Fig. 1a,b) involves the rotation of a bead by a random angle. The rotation of a central bead conserves the central bond angle and the lengths of the adjacent bond vectors, while the rotation of an end vector just conserves its length. The "sliding" move (Fig. 1c) consists of the virtual cutting of the model chain at one point, making an end-type rotation at that point and then rebuilding the cut fragment starting from the rotated point. This last move affords the possibility of moving large fragments of the molecule over a short distance without disrupting the internal structure of the fragment undergoing the motion.

In order to calculate the transition probability, we require the energy as a function of the chain conformation and its location in space. In the present model, this energy consists of two classes of terms—the internal energy of the amino acid which depends on the local conformation of the peptide, and coupling terms which mimic the presence of the lipid and water phases; therefore, they depend on the position of the amino acid in the Monte Carlo box.

The internal energy of a given bead is a function of the bond angle  $\theta$  and the torsional angle  $\rho$  (see Fig. 2). Since the model is designed to simulate helical peptides, both potentials are approximated by a function having a single minimum at  $\theta_0 = 89^\circ$  and  $\rho_0 = 52^\circ$ . These values are chosen to reproduce the positions of the C- $\alpha$  carbons in an ideal  $\alpha$ -helix and are obtained from Barlow and Thornton.<sup>20</sup> This canonical  $\alpha$ -helix is characterized by the backbone dihedral angles:  $\phi = 62^\circ$  and  $\psi = -41^\circ$ .

An essential feature of this model is the interaction of an amino acid with its environment. There are several hydrophathy scales obtained on the basis of solubility and partitioning data for free amino acids and side chain analogues (see for example, the reviews in refs. 21 and 22). As Roseman has observed,<sup>17</sup> these scales very often are based upon the assumption that the transfer energy of an amino acid side chain is additive and that this energy is the

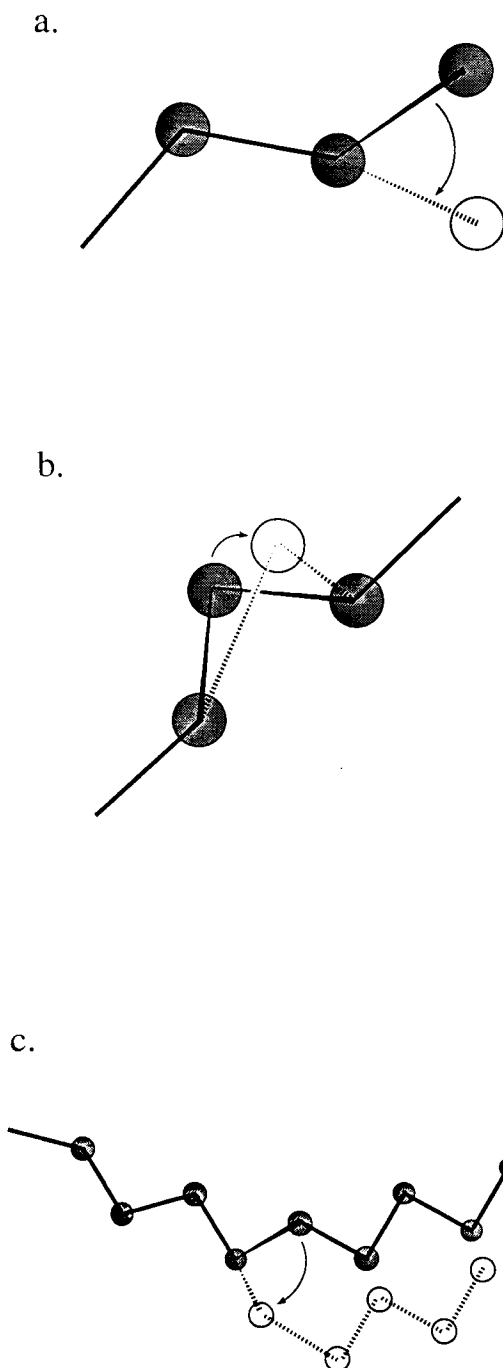


Fig. 1. An illustration of micro modifications used in the algorithm. (a) "Spike" move of the end vector; (b) "spike" move of an internal residue; (c) "sliding" move.

same for an individual amino acid and for an amino acid in a peptide chain. According to Roseman<sup>17</sup> this assumption is sometimes misleading. This is especially true for charged side chains, where the free energy of transfer from water into the hydrocarbon phase, according to some hydropathy scales, requires from 12 to 20 kcal/mol (1 kcal = 4.184 kJ).

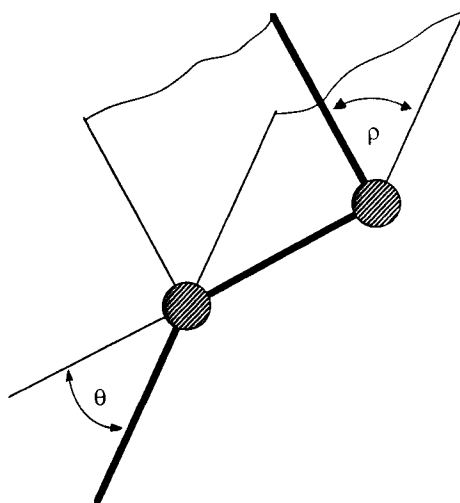


Fig. 2. Definitions of the bond angle  $\theta$  and the torsional angle  $\rho$ .

Roseman<sup>17</sup> proposed an experimentally derived scale based on water/octanol partition coefficients of *N*-acetyl amino acid amides. The free energies of transfer for polar amino acids so obtained are 40 to 85% less than those calculated assuming structure additivity. The hydropathy scale for side chains that we employ may be found in Table 3 of Roseman's paper.<sup>17</sup>

The next important fact which must be addressed is that the lipid bilayer is not uniform hydrophobic phase. The head-group region of a bilayer interface forms a very important part of the system, whose thermodynamic properties are different from the properties of the rest of the bilayer. Indeed, according to Jacobs and White<sup>4</sup> (JW), the adsorption of peptides onto the bilayer interface plays an important role in helix formation and insertion.

In order to accommodate these features, depending on the location of the peptide along the *z* axis, we divide our Monte Carlo box into five regions. As schematically shown in the top of Figure 3, the hydrophobic phase in the center of the MC box is surrounded by two head group layers and two water layers. The bottom part of this figure presents the fraction of "water phase" (dashed line) and "hydrocarbon phase" (dotted line) in the Monte Carlo box as a function of the *z*-coordinate. We have used a  $1/[1 + \exp(2z)]$  type function to model the border between phases; this produces a smooth transition between the various phases.

The detailed shape of the function depicting the interface of the bilayer is not crucial at the level of abstraction in the present model. One has to remember that the model is based on a  $C\alpha$  representation of amino acids and a very schematic representation of the lipid phase. The transition function was here used only for smoothing the borders between phases

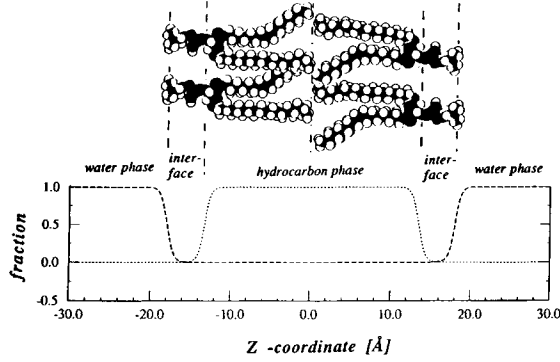


Fig. 3. Schematic illustration of composition of the Monte Carlo box in the present model. The MC-box is divided according to the position along the z-axis into five phases. The phases are defined using the percentage of "water" and "hydrocarbon" for a given value of z-coordinate, as it is presented in the bottom fragment of the figure.

and was chosen from the point of view of algorithmic convenience rather than for rendering the exact details of the structure of the fluid bilayer. However, we have tested the influence of changes of shape of the interfaces on the dynamics of the model, and we find that too sharp interfaces makes the insertion of the peptide into bilayer very difficult. The model chain has less space for preparing of fragments of secondary structure, which can be then transported into the hydrocarbon phase.

The walls of the Monte Carlo box are impenetrable for peptide chains, and the box is large enough to give the peptide chain the possibility to diffuse and freely change its conformation.

Following JW,<sup>4</sup> the process of transfer of an extended peptide chain from water to the bilayer is divided into two main steps: (1) the transfer from water into the head group phase; and (2) the transfer from the head group phase into the hydrocarbon phase.

The free energy of transfer of a peptide from water to the interface  $\Delta G_{w \rightarrow if}$  can be represented using Eq. (11) of the JW paper.<sup>4</sup>

$$\Delta G_{w \rightarrow if} = \Delta G_{ifh} + \Delta G_{imm} \quad (1)$$

where  $\Delta G_{ifh}$  is the free energy of transfer associated with the partial burial of the extended chain in the lipid phase when it is constrained to lie in the interface and is defined according to Eq. (10) of JW<sup>4</sup>,

$$\Delta G_{ifh} = f \Delta G_{fob} = f C_s A_s \quad (2)$$

where  $f$  is the fractional area of the peptide that is buried at the interface,  $C_s$  is a solvation parameter, and  $A_s$  is the total accessible surface area of the peptide in an extended conformation.<sup>23</sup> We have assumed in the present simulation that  $f=0.56$  and  $C_s = -22.0 \text{ cal}/(\text{mol} \cdot \text{\AA}^2)$ , according to JW.<sup>4</sup>

$\Delta G_{imm}$  is the change in free energy due to the reduction in the external degrees of freedom of a

peptide when the peptide is constrained to lie on a surface. It represents an unfavorable water-to-interface transport free energy. Being very difficult to evaluate using analytical methods,<sup>1,2,4</sup> it was neglected in the JW analysis. The present Monte Carlo simulation scheme, at least, accounts for the entropic contributions to  $\Delta G_{imm}$ .

Burial of a peptide disrupts the lipid packing and thereby the orientational order of the lipid. To account for the lipid perturbation effect in our model, we introduce a standard nematic type potential,  $\Delta G_{lip}$ . In the simplest version, this change depends on the orientation of the peptide fragment relative to the main ordering axis of the lipid phase (which is presumed to be perpendicular to the surface). In the model, this energy is calculated according to

$$\Delta G_{lip} = C_{ord} \times \sin^2(\theta) \quad (3)$$

where  $C_{ord}$  is a coefficient, and  $\theta$  is the angle between the end-to-end vector of a polypeptide fragment consisting of four residues, and the normal to the membrane surface.  $C_{ord}$  is chosen to be relatively small and assumes values from 0.05 to 0.15 kcal/residue. This realization of the lipid perturbation energy was first successfully used in our earlier lattice model of insertion of peptide chains into a bilayer.<sup>16</sup>

The free energy of transport of a peptide fragment in a nonhelical conformation from the interface to the interior of a bilayer ( $\Delta G_{ext}$ ) is defined analogous to Eq. 16 of JW:

$$\Delta G_{ext} = (1-f)C_s A_{Gly} + \Delta G_{bb} + \Delta G_{sc} \quad (4)$$

where  $A_{Gly}$  is the accessible surface area of a glycine residue.

$(1-f)C_s A_{Gly}$  denotes the residual transfer free energy, which was not satisfied upon attachment at the interface and is calculated for the glycine residue (this term will be discussed below);

$\Delta G_{bb}$  is the free energy of transfer of backbone polar groups which are not hydrogen bonded;

$\Delta G_{sc}$  is the corrected, self-solvation transfer free energies for whole side chains, obtained from Table 3 of the Roseman paper.<sup>17</sup>

We define the  $\Delta G_{sc}$  term somewhat differently from the treatment of JW. In the original JW definition, this was the free energy of transfer of the polar groups of the side chain. Because the side chain transfer free energy from the water to the lipid phase is now included in  $\Delta G_{sc}$ , we use the hydrophobic free energy for glycine to account for the backbone transfer free energy in which polar backbone interactions are excluded. For  $\Delta G_{bb}$ , JW have used 6.12 kcal/mol, which is an upper limit for this value.<sup>4</sup> Here, we have decreased this value to 4.1 kcal/mol (about 2/3 of the JW value) to account for

**TABLE I. Values (in kcal/mol) of the Free Energy of Transport of Amino Acids in Nonhelical ( $\Delta G_{\text{ext}}$ ) and Helical ( $\Delta G_{\text{hlx}}$ ) Conformations, From the Interface to the Interior of a Bilayer**

Residue	$\Delta G_{\text{ext}}$	$\Delta G_{\text{hlx}}$
A	2.58	-0.82
C	1.25	-2.05
D	4.82	1.82
E	5.03	2.53
F	0.01	-3.09
G	3.25	-0.55
H	4.34	1.54
I	0.23	-3.17
K	5.71	2.31
L	0.23	-2.97
M	1.58	-1.92
N	5.52	2.62
P	-1.10	-0.60
Q	5.37	2.27
R	7.14	3.64
S	3.35	-0.05
T	2.83	-0.57
V	1.07	-2.33
W	0.39	-2.81
Y	4.23	1.63

the self-solvation effect, according to Roseman.<sup>17</sup> The Pro residue is the only exception where we use  $\Delta G_{\text{bb}} = 1.5$  kcal/mol because of its specific structure. The values of  $\Delta G_{\text{ext}}$  obtained using Eq. 4 for all the residues are presented in the Table I.

The free energy of transport of a peptide residue in the helical conformation ( $\Delta G_{\text{hlx}}$ ) is defined by

$$\Delta G_{\text{hlx}} = \Delta G_{\text{ext}} + \Delta G_{\text{bH}} + \Delta G_{\text{lost}} \quad (5)$$

where  $\Delta G_{\text{bH}}$  is the free energy associated with the formation of backbone hydrogen bonds;  $\Delta G_{\text{lost}}$  is the decrease of side chain hydrophobicity due to change of the accessible surface area of side chains during formation of an  $\alpha$ -helix from an extended conformation.

The free energy of hydrogen bond formation is estimated by JW<sup>4</sup> to be  $-5.57$  kcal/mol. In order to consider the self-solvation effect, we decrease this value to  $-3.8$  kcal/mol, about  $\frac{2}{3}$  of the JW value, analogous to what we did for the  $\Delta G_{\text{bb}}$ . The  $\Delta G_{\text{hlx}}$  potential works complementary to the structural propensities defined above as  $E_{\text{bond}}$  and  $E_{\text{tors}}$  and has a comparable value (see Table II). We use both the potentials, because the structural propensities can distinguish between left- and right-handed helices and  $\Delta G_{\text{hlx}}$  is environment sensitive and prefers the lipid phase. The values for the approximate loss of side chain hydrophobicity due to formation of an  $\alpha$ -helix are taken from Table 4 of Roseman's paper.<sup>17</sup>

The hydrogen bond energy obviously depends on

**TABLE II. The Values of Parameters Used for the Simulations Presented in This Paper**

Parameter	Value
Temperature	305.0 (K)
Minimum of the bond potential [ $E_{\text{bond}}(\theta_0)$ ]	2.0 (kcal/mol)
Equilibrium bond angle ( $\theta_0$ )	89.5 (deg)
Minimum of the torsional potential [ $E_{\text{tors}}(\rho_0)$ ]	1.5 (kcal/mol)
Equilibrium torsional angle ( $\rho_0$ )	52.1 (deg)
Nematic potential coeff. [ $C_{\text{ord}}$ in Eq. (3)]	0.05 (kcal/mol)
Thickness of the hydrocarbon phase (see Fig. 3)	27.0 (Å)
Thickness of the interface (see Fig. 3)	4.5 (Å)

the conformation of the peptide fragment. To account for this effect in our model, we have defined an additional function,

$$f_{\text{Hb}} = 1 - f_1(r_{i,i+3}) + f_2(r_{i,i+4})$$

which has the values from 0 to 1. The functions  $f_1$  and  $f_2$  are defined according to the equation

$$f_j = a_j + x^4 / (0.1 + x^4)$$

with  $j=1$  or 2.  $a_j$  is a constant that shifts the maximum in  $f_1$  to  $r_{i,i+3} = 5.04$  Å and the maximum in  $f_2$  to  $r_{i,i+4} = 6.3$  Å. These distances are characteristic of those in helices according to Barlow and Thornton.<sup>20</sup>

Values of  $\Delta G_{\text{hlx}}$  obtained using Eq. 5 are presented in Table I. Having these values, we can calculate the energy of a given residue in a given conformation and environment. The final formula for calculation of the value of the free energy is

$$\Delta G = -f_{\text{water}}\Delta G_{\text{w} \rightarrow \text{if}} + f_{\text{hc}}[\Delta G_{\text{ext}} + f_{\text{Hb}}(\Delta G_{\text{bH}} + \Delta G_{\text{lost}}) + \Delta G_{\text{lip}}] \quad (6)$$

where  $f_{\text{water}}$  and  $f_{\text{hc}}$  are the fractions of water and hydrocarbon defined by  $z$ -coordinate dependent functions, presented in Fig. 3, and the remainder of the symbols are defined above. Figure 4 shows as an example the free energy of methionine residue as a function of the  $z$ -coordinate. The solid line represents the free energy of the residue in an extended conformation, and the dotted one is the free energy in a helical conformation. The actual value of  $\Delta G$  (for the hydrocarbon region) lies between these two values and depends on the function  $f_{\text{hc}}$  (the local conformation of the peptide).

## RESULTS

### Simulation of Amphipathic Helical Peptides

Two membrane peptides, Magainin2 and M28, were used in the initial simulations. The sequences and information about their properties were taken

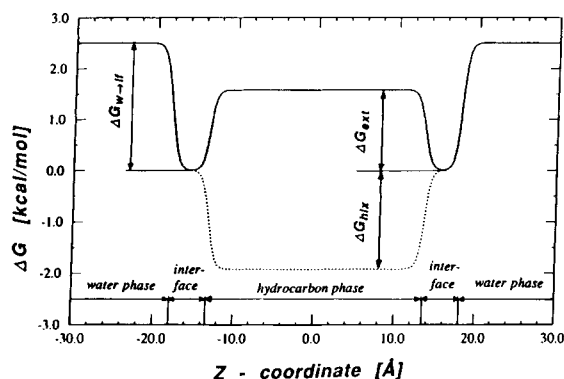


Fig. 4. Free energy of a methionine residue plotted as a function of its  $z$ -coordinate. The solid line denotes a nonhelical conformation and the dotted line an  $\alpha$ -helical conformation.

from the paper of Bechinger et al.<sup>24</sup> Magainin2 is a member of a family of 21–26 residue peptides found in the skin of frogs.<sup>25</sup> Magainins have antibacterial activities, but do not lyse red blood cells.<sup>24</sup> NMR experiments indicate that magainins are predominantly helical in detergent micelles<sup>26</sup> and unfolded in water. The Magainin2 used in the simulation has the sequence<sup>24</sup>:

**GIGKFLHSAKKFGKAFVGEIMNS**

(the hydrophobic amino acids are bold; the charged amino acids are in italics). An analysis of solid-state NMR spectra showed that this peptide is adsorbed on the surface of the bilayer.<sup>24</sup>

The M28 peptide has the sequence<sup>24</sup>:

**EKMSTAISVLLAQAVFLLLSQR**

(again, the hydrophobic amino acids are bold; the charged amino acids are in italics). This peptide differs from Magainin2 in both the pattern of hydrophobes and hydrophils and its physiological activity.<sup>24</sup> In the Magainin2 sequence, charged and hydrophobic amino acids are mixed according to an amphipathic helix motif. The amino acid composition and pattern of M28 is close to those of signal sequences<sup>27</sup>; the hydrophobic side chains are clustered in the middle of the sequence. M28 lipid lyses red blood cells<sup>28</sup> and forms a transmembrane helical structure in bilayers.<sup>24</sup>

These peptides were used as the first test of our model. Both simulations started from the same initial unfolded conformation in the aqueous phase and used the same set of initial parameters. Table II contains the set of parameters used for the simulation of Magainin2 and M28 peptides.

Figure 5 contains some representative snapshots from the simulation trajectory of Magainin2. The simulation started from a randomly coiled peptide chain in water (Fig. 5a). After a short time, the chain adsorbs on the membrane surface (Fig. 5b). It first forms a slightly disrupted (Fig. 5c), and then an

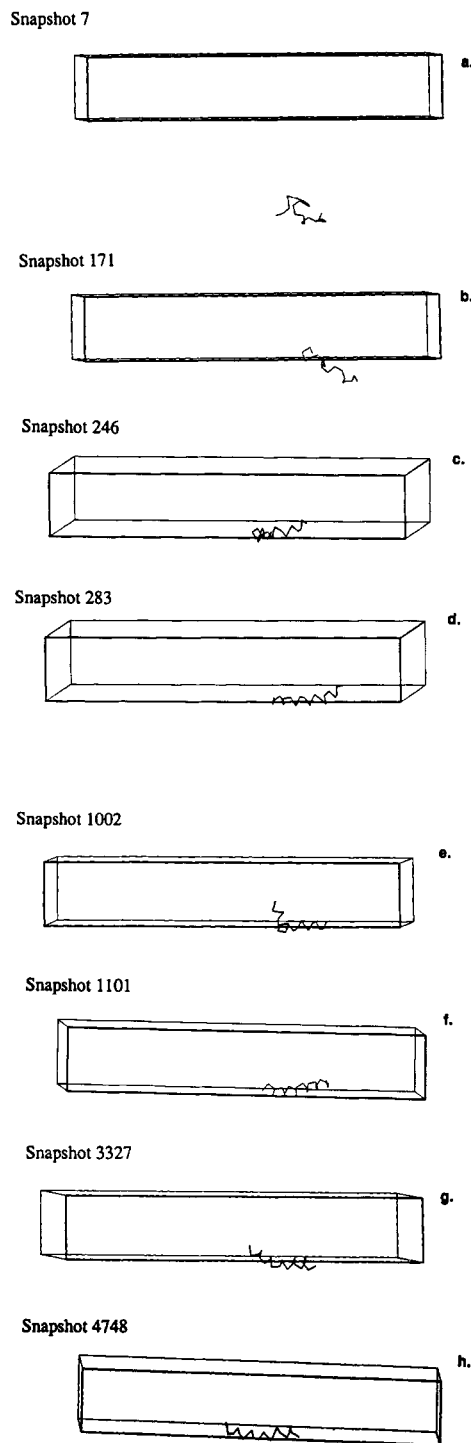


Fig. 5. Snapshots from one of the simulations of Magainin2. The box indicates the lipid phase. See text for comments and further details.

ordered (Fig. 5d) helical structure. Magainin2 remains adsorbed on the membrane surface, and the helical structure persists during the rest of the simulation. The structure is not frozen, and the adsorbed chain has the possibility of diffusing on the

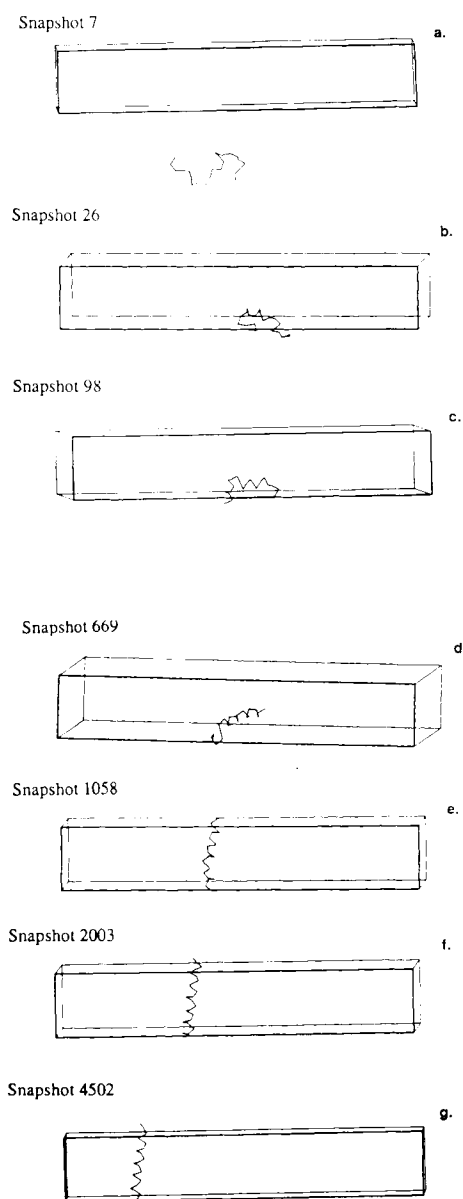


Fig. 6. Snapshots from one of the simulations of M2d peptide. The box indicates the lipid phase. See text for comments and further details.

membrane surface. As shown in Figure 5e, both ends of the peptide chain can partially insert into the hydrocarbon phase. However, this is a very unstable conformation which rapidly dissolves (Fig. 5f). The two next snapshots (Fig. 5g,h) show that the system remains stable during the rest of a long simulation.

Figure 6 shows analogous snapshots of the M2 $\delta$  simulation. The peptide chain, initially located in the water chain (Fig. 6a), adsorbs at the membrane surface (Fig. 6b) and forms a helical structure close to the surface of the membrane. The central frag-

ment of the M2 $\delta$  peptide is mostly hydrophobic; therefore, the structure looks like a "bridge," with both of its hydrophilic ends on the surface and the hydrophobic interior buried in the hydrocarbon phase (Fig. 6c). This structure requires disruption of the helical structure at two points and is energetically unfavorable. The best conformation of the system is one where both ends are on surface, the central point is in hydrocarbon phase, and the structure is fully helical. This is possible only for a transmembrane helix, but the transition from the "bridge like" adsorbed structure to the trans-bilayer conformation requires the system to cross an energetic barrier. The intermediate conformation, where the helical structure is partially disrupted and one of the hydrophilic ends is buried in the hydrocarbon phase (Fig. 6d), has a high energy. The system makes a few attempts to cross this barrier, and finally forms a trans-bilayer structure (Fig. 6e). This structure can laterally diffuse in the membrane, but remains stable in sense of orientation and overall conformation (Fig. 6f,g).

For both peptides, the simulations were repeated 12 times with changes in the random number generator seeds and the initial structures. In all cases, the results of the simulations are consistent with experimental data. The model of Magainin2 forms a helical structure which lies on the surface of the lipid phase, and the model of M2 $\delta$  forms a trans-bilayer helix. Note that the chains are not frozen; they can diffuse in the membrane plane, but the orientation remains stable. In this sense, the molecules are in a broad, global minimum in conformational space.

To quantitate information about the structure and orientation of these peptides, we have measured the mean over trajectories of the  $z$ -coordinates of the C $\alpha$ s for both chains. The resulting curves, showing the mean  $z$ -coordinates as a function of residue number, are presented in Figure 7a for Magainin2 and Figure 8a for M2 $\delta$ . Figures 7b and 8b show deviations in  $r_{i,i+3}$  and  $r_{i,i+4}$  (measured in Å) from the "ideal" helical values defined above,<sup>20</sup> as a function of the residue number. In both figure, the bars denote values of the mean absolute deviations defined by

$$S(x_1, \dots, x_N) = 1/N \sum |x_i - x_{\text{mean}}| \quad (7)$$

with  $x_i = r_{i,i+3}$  or  $r_{i,i+4}$  as appropriate.

The mean values of the  $z$ -coordinates for both peptides are very well defined, with the mean deviation almost always less than 2 Å. The Magainin2 helix is slightly curved with the N-terminus more buried in the hydrocarbon phase. What is important is that the helix does not rotate around its main axis. One side of the helix is always buried, while the other is exposed to water. The analysis of Figure 7b indicates that the structure of Magainin2 is slightly dis-



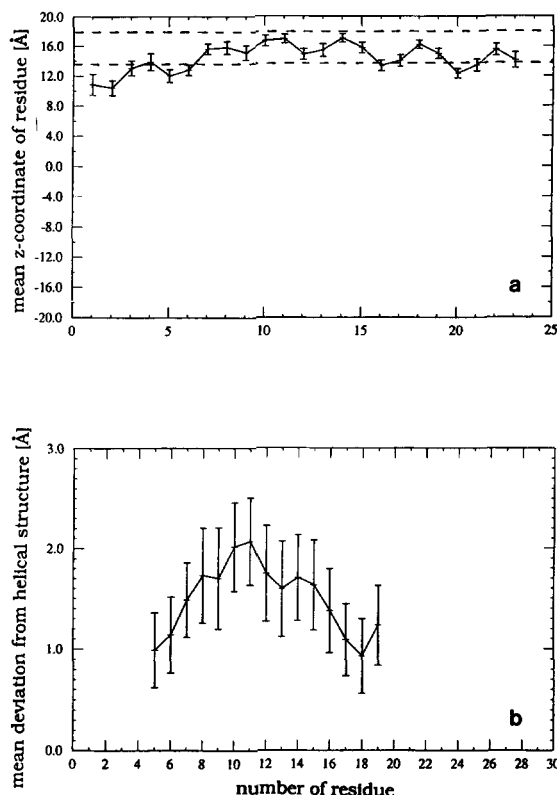


Fig. 7. Mean conformation and orientation parameters for Magainin2: (a) the mean z-coordinate of the residue; (b) the mean deviations from an "ideal" helical structure. The bars denote values of mean absolute deviations of the data (see definition in text).

torted and that this distortion is maximal in the central fragment of the chain.

Analysis of analogous curves for the model of M28 shows a different picture. The C $\alpha$ s have very well defined z-coordinates (Fig. 8a) and create an almost ideal trans-bilayer structure. The deviations from the mean helical structure (Fig. 8b) are very small; the structure is almost ideal in the center of the helix and is slightly distorted at both ends.

### Simulation of Melittin

Melittin is the major protein component of the venom of the European honey bee *Apis mellifera*. This is a 26 amino acid peptide having a powerful hemolytic activity<sup>29</sup> with the sequence:<sup>29</sup>

**GIGAVLKVLTTGLPALISWIKRKRQQ**

(as before, the hydrophobic amino acids are bold, and the charged amino acids are in italics). The N-terminus of melittin has a predominantly hydrophobic character. The C-terminus is very hydrophilic and basic. In spite of its overall hydrophobicity, melittin is soluble in both water and in methanol. In water, melittin can be monomeric or tetrameric. Monomeric melittin in water has no detectable secondary structure (Dempsey<sup>14</sup> and works cited there-

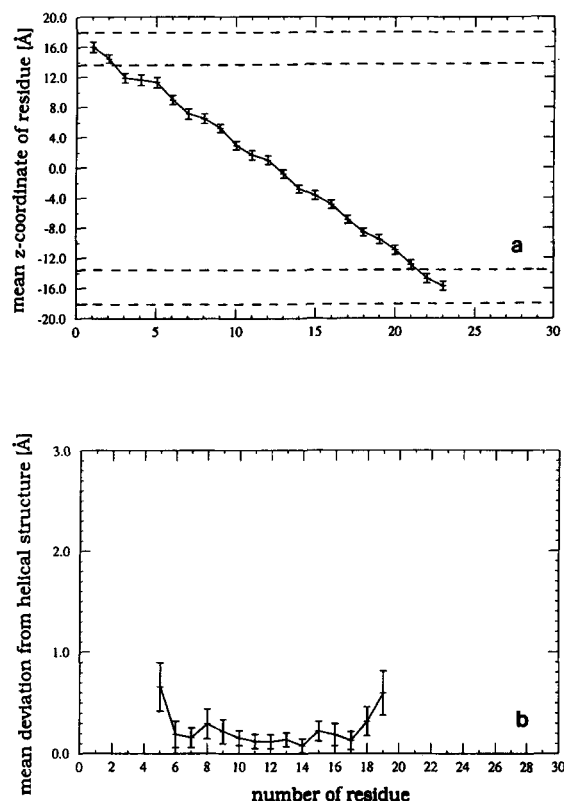


Fig. 8. Mean conformation and orientation parameters for M28 peptide in our model: (a) the mean z-coordinate of the residue; (b) the mean deviations from an "ideal" helical structure. The bars denote values of mean absolute deviations of the data (see definition in text).

in); the structure of tetramers has been solved to a resolution of 2 to 2.5 Å by analysis of X-ray diffraction data from two crystal forms.<sup>30</sup> Melittin adopts a helical conformation in the tetrameric state with the hydrophobic side chains packed within the structure. The helix in the tetrameric structure is bent with an angle of about 60° near Leu-13 and Pro-14. Using NMR spectroscopy it has been shown that, in methanol, melittin is monomeric and helical.<sup>31</sup> The difference between the water-tetramer structure and the methanol structure lies mainly in the structure of the bend fragment; the bend angle is about 20° in methanol. NMR, CD, and Raman studies of melittin indicate that the peptide is helical in a lipid environment.

The experimental situation concerning the orientation of melittin in a lipid bilayer is not so clear. A review of literature concerning this subject can be found in the work of Dempsey.<sup>29</sup> Vogel and Jahnig<sup>32</sup> measured the melittin helix orientation in the gel phase of ditetradecylphosphatidylcholine or dimyristoyl phosphatidylcholine at low hydration levels and conclude that the helix is oriented roughly perpendicular to the bilayer surface. The results from total reflectance (ATR) IR spectroscopy analysis on

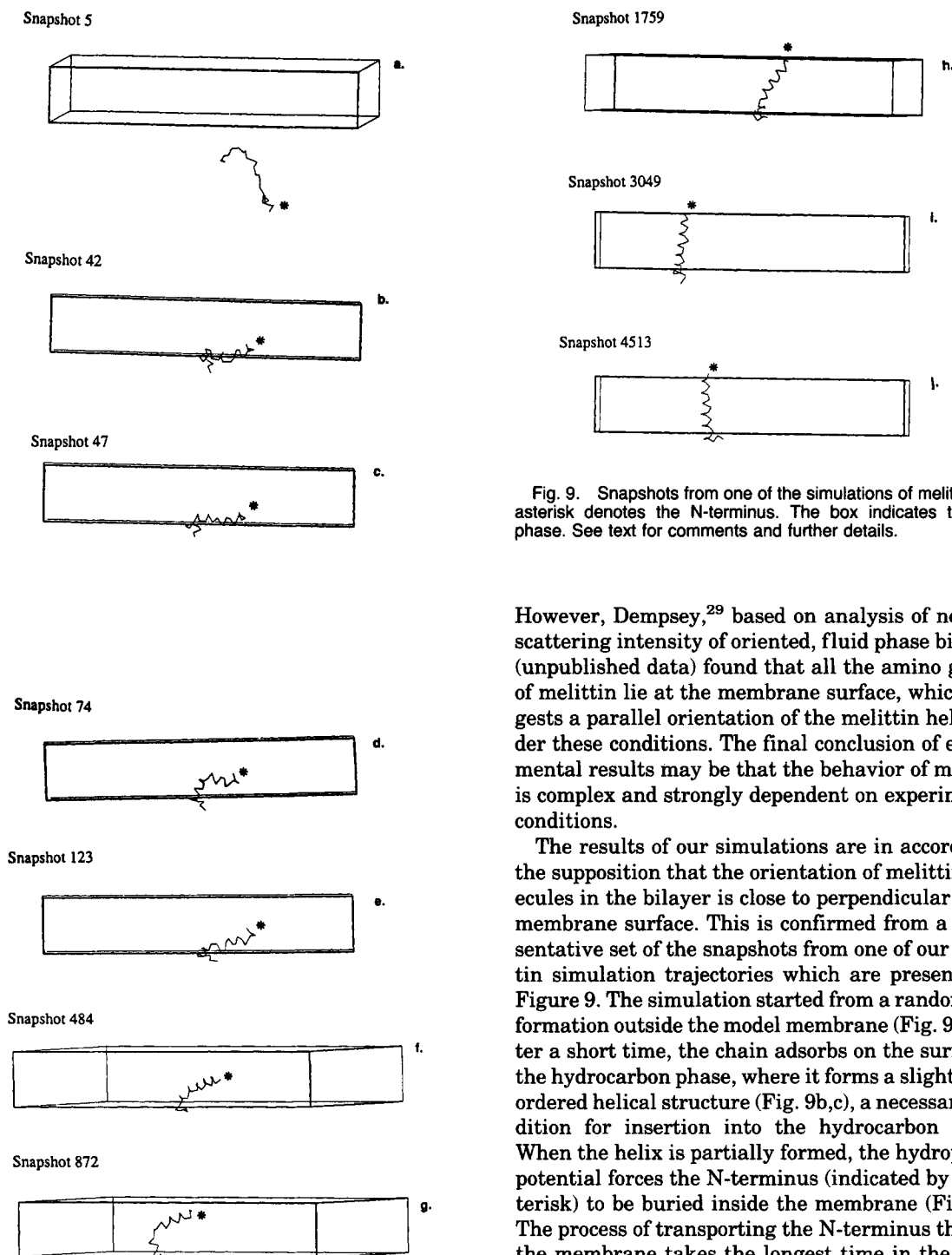


Fig. 9. Snapshots from one of the simulations of melittin. The asterisk denotes the N-terminus. The box indicates the lipid phase. See text for comments and further details.

However, Dempsey,<sup>29</sup> based on analysis of neutron scattering intensity of oriented, fluid phase bilayers (unpublished data) found that all the amino groups of melittin lie at the membrane surface, which suggests a parallel orientation of the melittin helix under these conditions. The final conclusion of experimental results may be that the behavior of melittin is complex and strongly dependent on experimental conditions.

The results of our simulations are in accord with the supposition that the orientation of melittin molecules in the bilayer is close to perpendicular to the membrane surface. This is confirmed from a representative set of the snapshots from one of our melittin simulation trajectories which are presented in Figure 9. The simulation started from a random conformation outside the model membrane (Fig. 9a). After a short time, the chain adsorbs on the surface of the hydrocarbon phase, where it forms a slightly disordered helical structure (Fig. 9b,c), a necessary condition for insertion into the hydrocarbon phase. When the helix is partially formed, the hydrophobic potential forces the N-terminus (indicated by an asterisk) to be buried inside the membrane (Fig. 9d). The process of transporting the N-terminus through the membrane takes the longest time in the insertion process. The N-terminus of melittin is hydrophobic, and there is only a weak tendency to make the main axis of the helix perpendicular to the surface. The tendency arises from the orienting forces in the peptide-lipid interaction and the polarity of the peptide terminus due to unsaturated hydrogen bonds. The net result is that the melittin chain "waves" in the membrane, with its orientation changing, as is shown in Figure 9e,f,g. Finally, after a long time, the N-terminus finds the opposite side

the orientation of melittin helices in dioleoylphosphatidylcholine and dipalmitoylphosphatidylcholine<sup>33</sup> and the analysis of CD spectra in oriented membranes and unoriented vesicles<sup>34</sup> also support the conclusion that the melittin helix is oriented approximately perpendicular to the bilayer surface.

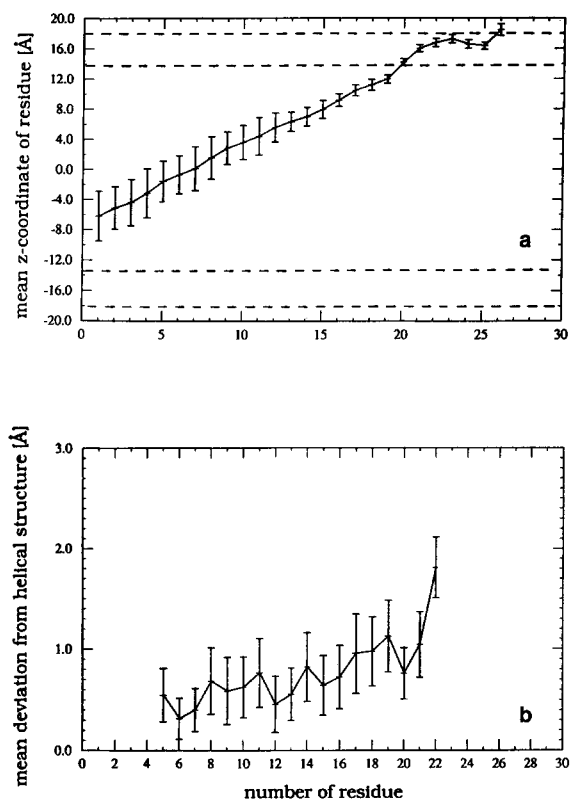


Fig. 10. Mean conformation and orientation parameters for melittin. (a) The mean z-coordinate of the residue; (b) the mean deviations from an "ideal" helical structure. The bars denote values of mean absolute deviations of the data (definition in text).

of the membrane (Fig. 9h), and the orientation of the molecule becomes more stable. The chain still has the possibility of diffusing, but the preferred orientation is perpendicular to the surface (Fig. 9i,j).

Analogous to Figures 7 and 8, Figure 10 parts a and b present the mean z-coordinate and the mean deviation from the "ideal" helix as a function of residue number. The mean z-coordinates for the model of melittin show that the chain never forms a trans-membrane structure; rather, the C-terminus floats on the interface. It is possible to distinguish two fragments in the chain: a stable fragment from the C-end of the peptide up to the Pro-14 residue, and the more mobile fragment from the Pro-14 to the N-terminus. The mobility of the residue can be estimated from the value of the mean absolute deviation of the z-coordinate of the residue. These conclusions are in good accord with NMR data and molecular dynamics simulation,<sup>14</sup> which indicate that the structure of melittin has two helical fragments connected by a more flexible fragment at Pro-14. The analysis of the deviations from an ideal helical structure (Fig. 10b) shows that the mobile, but buried N-terminal fragment is better defined than the surface anchored C-terminus. The simulations were repeated 12 times with different random num-

bers, and the same qualitative results were obtained.

The problem of orientation of melittin in the lipid bilayer phase is still open and we are waiting for new experimental data on this subject. Our rather schematic model prefers an orientation which is perpendicular to the surface, both the orientation of the real melittin may be an effect of more subtle thermodynamic parameters, which are not included here. We hope to return to this problem in our next, more realistic model of membrane-peptide systems.

### Simulation of Bacteriophage Pfl Coat Protein

Filamentous bacteriophage Pfl coat protein is an example of a simple membrane protein. It is secreted through the host cell membrane before it assembles around viral DNA.<sup>35</sup> NMR studies show that the structure of this 46 residue long protein contains two helices connected by a mobile linker.<sup>36</sup> The transmembrane hydrophobic helix contains residues from 19 to 42; the second helix runs from residues 6 to 13, is amphipathic, and lies on the surface of the membrane.

The Pfl coat protein was chosen as a test of the present model, because it is the simplest protein which contains both trans-bilayer and surface adsorbed helices. We asked the question, whether the algorithm can distinguish between these two regions using only information about sequence. To make this "numerical experiment" maximally pure, we have superimposed homogeneous helical propensities along the sequence. The goal of the calculation is not only to determine the orientation of the helix, but the position of the linker as well. This is even more difficult here than it is in nature, due to lack of the "turn-type" hydrogen bonds in the model, it costs the system free energy to disrupt the helical structure.

The amino acid sequence of the protein taken from the paper of Nakashima<sup>37</sup> is used. The set of snapshots in Figure 11, taken from one representative simulation, can provide insights into the behavior of the model protein. Every simulation started from a random structure outside of the membrane (Fig. 11a). In what follows, the N-terminus is marked by an asterisk. The chain diffuses for some time in the water phase where the propensities are too weak to form stable secondary structure (Fig. 11b). When the molecule contacts the membrane (Fig. 11c), it rapidly adsorbs on the surface and forms a long, unstable, quasi-helical structure (Fig. 11d). The more hydrophobic C-terminus fragment of the protein has a tendency to be inserted into the bilayer, but it must wait for a large enough energy fluctuation to transport the hydrophilic C-terminus through the bilayer. A "wrong variant" of the process is an insertion of a broken hydrophobic helix into the membrane (as in Fig. 11e,f,g). This structure is in a local energy minimum in the system, but it is almost im-

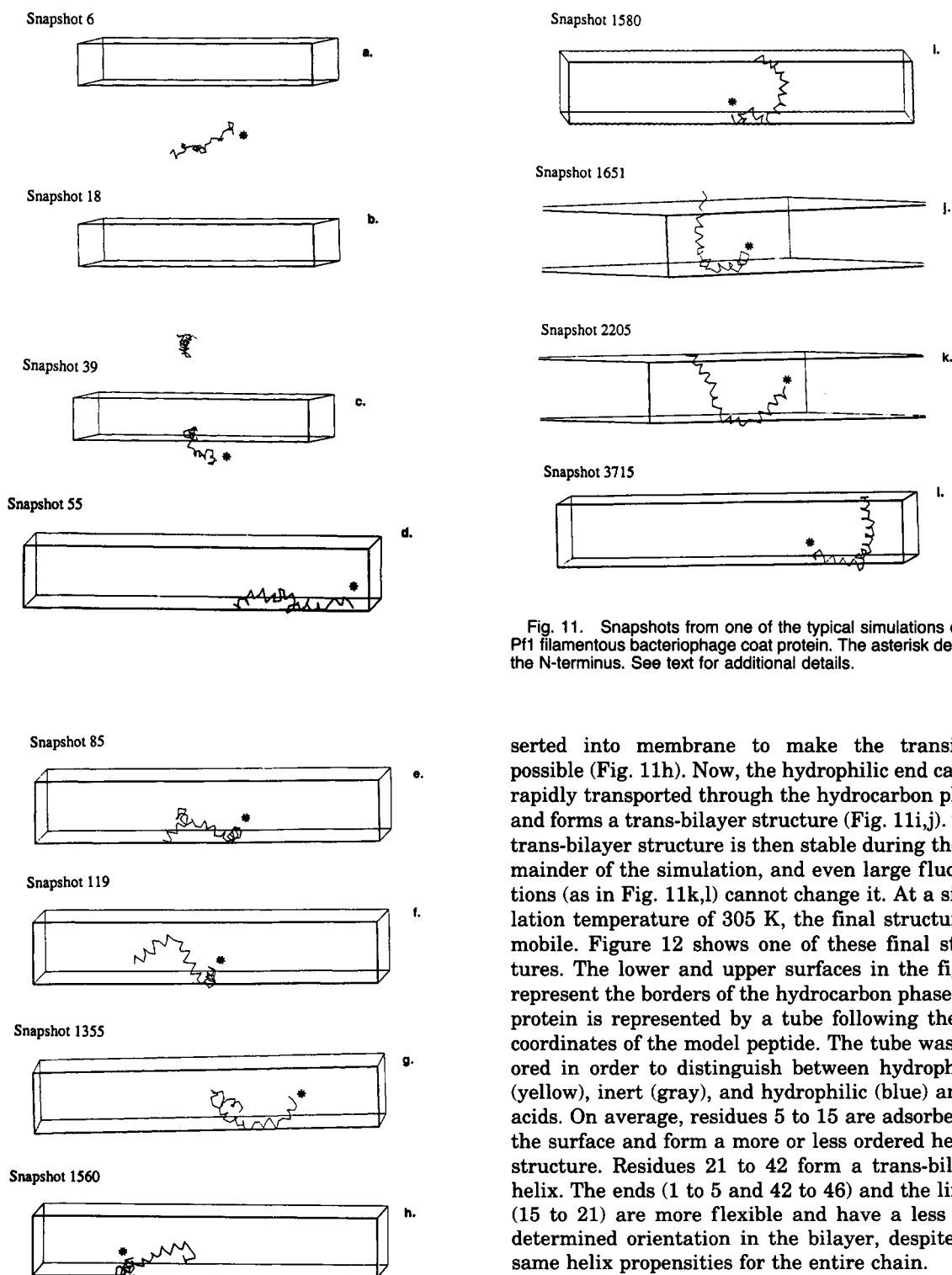


Fig. 11. Snapshots from one of the typical simulations of the Pf1 filamentous bacteriophage coat protein. The asterisk denotes the N-terminus. See text for additional details.

possible to reconstruct the transmembrane helix inside the membrane. Because the lack of hydrogen bonds in the lipid phase is energetically very expensive, a long fragment (almost all) of the trans-bilayer helix must be prepared on the surface and in-

serted into membrane to make the transition possible (Fig. 11h). Now, the hydrophilic end can be rapidly transported through the hydrocarbon phase and forms a trans-bilayer structure (Fig. 11i,j). This trans-bilayer structure is then stable during the remainder of the simulation, and even large fluctuations (as in Fig. 11k,l) cannot change it. At a simulation temperature of 305 K, the final structure is mobile. Figure 12 shows one of these final structures. The lower and upper surfaces in the figure represent the borders of the hydrocarbon phase; the protein is represented by a tube following the  $C\alpha$  coordinates of the model peptide. The tube was colored in order to distinguish between hydrophobic (yellow), inert (gray), and hydrophilic (blue) amino acids. On average, residues 5 to 15 are adsorbed on the surface and form a more or less ordered helical structure. Residues 21 to 42 form a trans-bilayer helix. The ends (1 to 5 and 42 to 46) and the linker (15 to 21) are more flexible and have a less well determined orientation in the bilayer, despite the same helix propensities for the entire chain.

The structural properties of the model of the Pf1 peptide can be analyzed analogous to previous cases, using values of the mean  $z$ -coordinates and deviations from the mean helical structure as a function of the residue number (Fig. 13a,b). These curves show that the fragment from the N-terminus to Lys-20 forms a slightly disordered helical structure adsorbed on the interface of the membrane. The C-

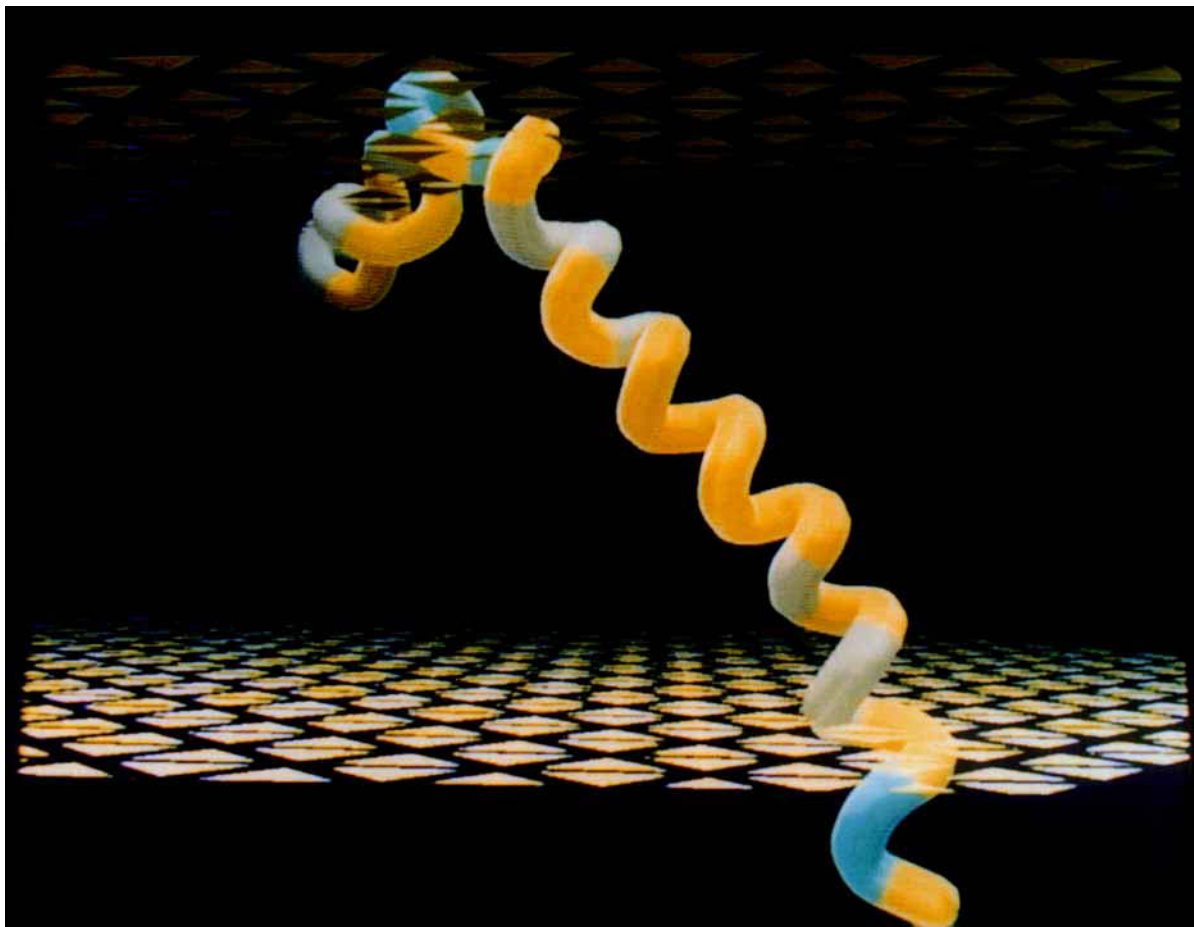


Fig. 12. A representative final structure of filamentous bacteriophage Pf1 coat protein obtained using the present model. The upper and lower surfaces on the figure represent borders of the hydrocarbon phase. The protein is represented as a tube fol-

lowing the  $C\alpha$  positions of the model chain. The yellow colored fragments of the tube denote hydrophobic amino acids, the blue color corresponds to the hydrophilic, and the gray to inert ones.

terminus fragment (from Gly-24) forms a very ordered (almost ideal), trans-bilayer, helix. These results are in good accord with experimental data<sup>36</sup> and provide one more example that the model can give a good prediction of the structure, orientation, and insertion mechanism of membrane peptides and short proteins.

The *in vivo* insertion path of the Pf1 coat protein is probably different from that presented here, because we expect that the native coat protein has an additional signal sequence, which is involved in the insertion process. The *in vivo* mechanism is probably initiated by formation of a helical hairpin adsorbed on the surface of the cell membrane. The hairpin consisting of a signal peptide and the N-terminus of the protein, inserts into the membrane phase and then pulls the rest of the protein with it. The signal sequence is then cleaved by the signal peptidase. This way, the N-terminus of the protein is

outside of the protein cell membrane, and the C-terminus is inside.<sup>35</sup> The simulation depicted in Figure 11 presents a possible *in vitro* mechanism of insertion of a mature protein into a bilayer. The insertion of the more hydrophobic C-terminus of the protein is kinetically easier than is the insertion of the amphipathic N-terminal helix. That is why in this model, the C-terminus crosses the membrane.

Figure 14 shows a sequence of snapshots from one of 12 simulations, which can illustrate a possible *in vivo* path of insertion of the Pf1 coat protein. The simulation started, as usual, from a random conformation in the water phase. The chain diffuses freely in the water phase, and due to random fluctuations achieves a needlelike conformation, almost perpendicular to the membrane surface, with the N-terminus adsorbed on it (Fig. 14a). Because the borders of the phases are not sharp in the present model, the hydrophobic residues of the N-terminal fragment

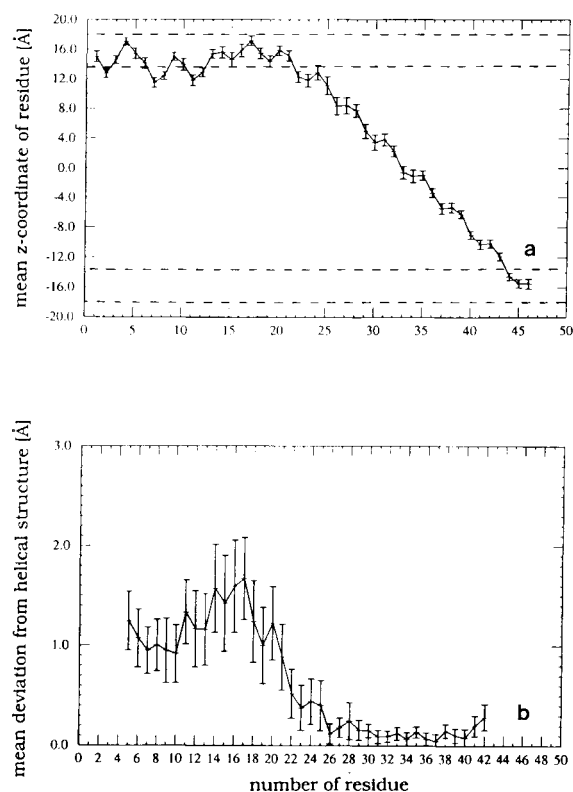


Fig. 13. Mean conformation and orientation parameters for the Pf1 filamentous bacteriophage coat protein. (a) The mean z-coordinate of the residue; (b) the mean deviations from an "ideal" helical structure. The bars denote values of mean absolute deviations of the data (definition in text).

"feel" the nearness of the hydrocarbon phase, and the chain is very quickly pulled into the membrane (Fig. 14b). This process is so fast that the chain has no time to change its orientation and punctures the membrane like a needle. The resulting conformation (Fig. 14c) is opposite to that in Figure 11, because the N-terminus of the protein forms a transmembrane helix while the C-terminus forms a surface adsorbed helical structure. The transition to global free energy minimum configuration is slower and is related to the transport of the chain across the membrane (Fig. 14d,e,f). The N-terminus helix become adsorbed on outside surface of the membrane, and the C-terminus forms a trans-bilayer helix (Fig. 14g,h,i).

This simulation indicates, at least for the model, that the N-terminus of the Pf1 coat protein can be transported through a cell membrane without a leader sequence or specific apparatus. The forces arising from the hydrophobic effect are sufficient to make this process possible. Probably, the efficiency of such a process is very low without any help from the cell transportation apparatus, and the structure from Figure 14c may be in reality arise due to a hydrophobic leader sequence (helical hairpin hy-

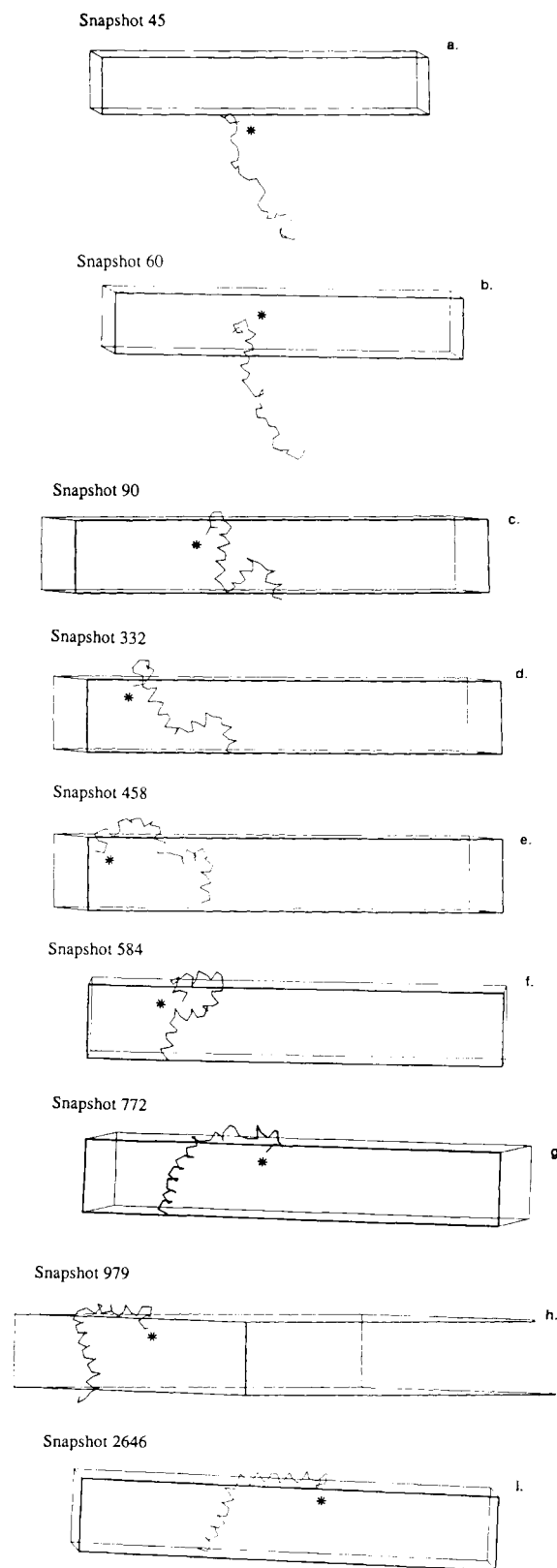


Fig. 14. Snapshots from the simulation of the Pf1 filamentous bacteriophage coat protein, where the N-terminus (denoted by an asterisk) is transported through the membrane. See text for additional details.

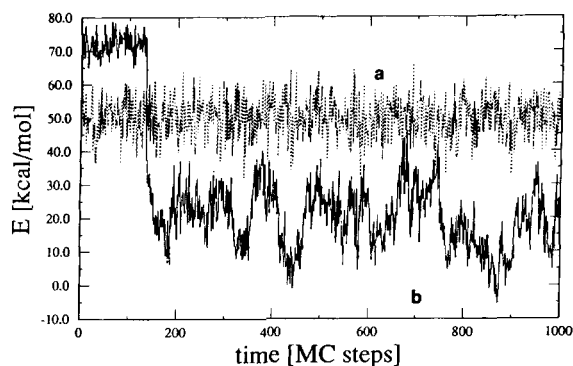


Fig. 15. Example illustrating the difference in behavior of our model system with different hydrophobicity scales. Plots of internal energy of the model M28 peptide as a function of time of simulation with (a) the JW scale and (b) with the scale proposed here. The original Roseman's without self-solvation effect gives analogous results to the JW scale.

pothesis) or a specialized cell apparatus, but the rest of the insertion process seen in Figure 14d–i may be realistic.

### CONCLUSION

The model presented here is a combination of hydropathy scale based methods for the prediction of trans-bilayer fragments in membrane proteins with dynamic Monte Carlo computer simulation techniques. The new hydropathy scale proposed here includes information about the multiphase structure of membrane-containing systems and experimental data about interactions of tripeptides with phospholipid membranes.<sup>4</sup> Starting from the JW<sup>4</sup> assumptions about the role of the membrane interface in the process of insertion of peptides and including the Roseman<sup>17</sup> considerations about the self-solvation effects, we have obtained a hydropathy scale which can be directly used in computer simulations.

Which particular hydrophobicity/polarity scale is appropriate for membrane proteins remains an open question, and our work on a very idealized model is not able to provide a quantitative evaluation of the thermodynamic properties of lipid–protein systems. Rather, we are interested in qualitative information about the conformation and orientation of peptides in membranes. Roseman's octanol partition data with self-solvation effect corrections were chosen because of a strictly pragmatic reason—they work in this present schematic model. Simulations using Jacobs and White's original scale, and the Roseman's scale without self-solvation effect corrections were unsuccessful. Because of very large values of  $\Delta G$  of transport of polar side chains from water into membrane phase, the chains could not insert into the hydrocarbon phase. Figure 15 shows a representative plot of the energy as a function of the simulation time for (a) the model of M28 peptide with the JW scale and (b) the scale presented in this paper. Use of

the original JW scale forces the chain to remain adsorbed on the membrane surface. System "a" is frozen and the fluctuations of energy are small relative to system "b." Simulations with the hydrophobicity scale proposed here resembles an all-or-none transition from an unfolded chain in the water phase to the transmembrane structure.

The Monte Carlo Dynamics method is used here to minimize the free energy of the system. Our approach couples the interaction energy of peptides with the phospholipid membranes to the local conformation and orientation of the peptide chain. The combination of the thermodynamic experimental data with stochastic simulations can give better insight not only into the structure of membrane proteins but also into the mechanism of insertion and transportation of membrane peptides. Additionally, since dynamic Monte Carlo procedures act to minimize the free energy, entropic contributions to the peptide insertion process are also included.

The simulations for the Magainin2 and M28 peptides demonstrate that the proposed model starting only from the peptide sequence can distinguish between trans-bilayer and surface-adsorbed helical structures. The mean  $z$ -coordinates of the residues and the mean deviation from the ideal helical structure give insights into the preferred conformation of the peptide and its orientation in the membrane. The results of the simulations are in accord with the experimental data for these molecules. Additionally, since the insertion mechanism is very reproducible, it may well be that this path is physical, and at the very least, it schematically imitates the real process. The insertion scheme for a trans-bilayer peptide, proposed here, consists of two stages:

1. adsorption on the surface of a membrane with concomitant formation of helical structure,
2. insertion of the preformed helix into the membrane mainly by rotation of the helix about an axis which is perpendicular to the helix principal axis and located near one of its ends.

Thus, the Engelman–Steitz<sup>1</sup> helix insertion hypothesis, as extended by Jacobs and White,<sup>4</sup> is supported by these simulations.

Our simulations of melittin support the conclusion that this molecule under normal conditions is oriented predominantly perpendicular to the membrane surface. The analysis of the trajectories of the insertion process shows that the melittin molecule is roughly divided into two helices connected by a linker near the residue Pro-14. The helical fragment closer to the N-terminus of the molecule is more mobile and is more likely to change orientation relative to the membrane surface, and the C-terminus helix, anchored in the interface, is more stable and mostly perpendicular to the surface.

The results from the Pfl coat protein simulations show that the present model can be successfully

used to simulate the folding of fragments larger than a single trans-bilayer helix (20–25 residues). Pfl coat protein is 46 residues long and contains both transmembrane type and amphipathic motifs in the sequence. The very good agreement of the simulation results presented above with experimental data opens up the possibility that the model may be used for structure prediction of large molecules, when it is extended to include explicit tertiary interactions between side chains. The analysis of the mechanism of insertion of the Pfl coat protein into a membrane shows that the transportation of the N-terminus across the bilayer may be of key importance. In these simulations, transport of the N-terminus across the bilayer is followed by the apparently irreversible transport of the amphipathic and turn fragments of the molecule and insertion of the trans-bilayer helix. The initial transportation of the N-terminus of the protein can be spontaneous (as occurred in one of the simulations) or it may be assisted by a hydrophobic leader sequence and/or by the cell transport apparatus.

We want to emphasize that, at this point, our simulations deal with monomeric peptides and can only be used for the description of the properties of very dilute peptides, where chain–chain interactions can be neglected. The more complicated model with chain–chain interactions is now being developed.

### ACKNOWLEDGMENTS

This work was supported in part by Grant GM-37408 for the Division of General Medical Sciences of the National Institutes of Health. Computing resources provided by Johnson & Johnson are gratefully acknowledged.

### REFERENCES

- Engelman, D.M., Steitz, T.A. The spontaneous insertion of proteins into and across membranes: The helical hairpin hypothesis. *Cell* 23:411–422, 1981.
- Jahnig, F. Thermodynamics and kinetics of protein incorporation into membranes. *Proc. Natl. Acad. Sci. U.S.A.* 80:3691–3695, 1983.
- Jacobs, R.E., White, S.H. Lipid bilayer perturbations induced by simple hydrophobic peptides. *Biochemistry* 26: 6127–6134, 1987.
- Jacobs, R.E., White, S.H. The nature of the hydrophobic binding of small peptides at the bilayer interface: Implications for the insertion of transbilayer helices. *Biochemistry* 27:3421–3437, 1989.
- Laine, R.O., Esser, A.F. Detection of refolding conformers of complement protein C9 during insertion into membranes. *Nature (London)* 341:63–65, 1989.
- Lazdunski, C.J., Benedetti, H. Insertion and translocation of proteins into and through membranes. *FEBS Letters* 268(2):408–414, 1990.
- Muller, G., Zimmermann, R. Import of honeybee pre-melittin into the endoplasmic reticulum: Energy requirements for membrane insertion. *EMBO J.* 7:639–648, 1988.
- Oliver, D.B., Cabelli, R.J., Jarosik, G.P. SecA protein: Autoregulated initiator of secretory precursor protein translocation across the *E. coli* plasma membrane. *J. Bioenerget. Biomembranes* 22(3):311–36, 1990.
- Parker, M.W., Tucker, A.D., Tsernoglou, D., Pattus, F. Insights into membrane insertion based on studies of colicins. *TIBS* 15:126–129, 1990.
- San Millan, J.L., Boyd, D., Dalbey, R., Wickner, W., Beckwith, J. Use of phoA fusions to study the topology of the *Escherichia coli* inner membrane protein leader peptidase. *J. Bacteriol.* 171(10):5536–41, 1989.
- van der Goot, F.G., Gonzalez-Manas, J.M., Lakey, J.H., Pattus, F. A “molten-globule” membrane-insertion intermediate of the pore-forming domain of colicin A. *Nature (London)* 354:408–410, 1991.
- Edholm, O., Johansson, J. Lipid bilayer polypeptide interactions studied by molecular dynamics simulation. *Eur. Biophys. J.* 14:203–209, 1987.
- Edholm, O., Jahnig, F. The structure of a membrane spanning polypeptide studied by molecular dynamics. *Biophys. Chem.* 30:279–292, 1988.
- Pastore, A., Harvey, T.S., Dempsey, C.E., Campbell, I.D. The dynamics properties of melittin in solution: Investigations by NMR and molecular dynamics. *Eur. Biophys. J.* 16:363–367, 1989.
- Milik, M., Kolinski, A., Skolnick, J. Monte Carlo studies of an idealized model of a lipid-water system. *J. Phys. Chem.* 96:4015–4022, 1992.
- Milik, M., Skolnick, J. Spontaneous insertion of polypeptide chains into membranes. A Monte Carlo model. *Proc. Natl. Acad. Sci. U.S.A.*, in press.
- Roseman, M.A. Hydrophilicity of polar amino acid side-chains is markedly reduced by flanking peptide bonds. *J. Mol. Biol.* 200:513–522, 1988.
- Gregoret, L.M., Cohen, F.E. Novel method for the rapid evaluation of packing in protein structures. *J. Mol. Biol.* 211:959–974, 1990.
- Binder, K., ed. “Applications of the Monte Carlo Method in Statistical Physics.” Heidelberg: Springer-Verlag, 1984.
- Barlow, D.J., Thornton, J.M. Helix geometry in proteins. *J. Mol. Biol.* 201:601–619, 1988.
- Fasman, G.D., Gilbert, W.A. The prediction of transmembrane protein sequences and their conformation: an evaluation. *TIBS* 15:89–92, 1990.
- Degli Esposti, M., Crimi, M., Venturoli, G. A critical evaluation of the hydrophathy profile of membrane proteins. *Eur. J. Biochem.* 190(1):207–219, 1990.
- Lesser, G.J., Lee, R.H., Zehfus, M.H., Rose, G.D. Hydrophobic interactions in proteins. *Prot. Eng.* 14:175–179, 1987.
- Bechinger, B., Kim, Y., Chirlian, L.E., Gessel, J., Neumann, J.-M., Montal, M., Tomich, J., Zasloff, M., Opella, S.J. Orientations of amphiphilic helical peptides in membrane bilayers determined by solid-state NMR spectroscopy. *J. Biomol. NMR* 1:167–173, 1991.
- Zasloff, M. Maginins, a class of antimicrobial peptides form *Xenopus* skin: Isolation, characterization of two active forms, and partial cDNA sequence of a precursor. *Proc. Natl. Acad. Sci. U.S.A.* 84:5449–5453, 1987.
- Shon, K., Zasloff, M., Opella, S.J. Unpublished results, 1991.
- von Heijne, G., Abrahmsen, L. Species-specific variation in signal peptide design: Implications for protein secretion in foreign hosts. *FEBS Lett.* 244:439–446, 1989.
- Kersh, G.J., Tomich, J.M., Montal, M. The M2δ transmembrane domain of the nicotinic cholinergic receptor forms ion channels in human erythrocyte membranes. *Biochem. Biophys. Res. Commun.* 162:352–356, 1989.
- Dempsey, C.E. The actions of melittin on membranes. *Biochim. Biophys. Acta* 1031:143–161, 1990.
- Terwilliger, T.C., Waissman, L., Eisenberg, D. The structure of melittin in the form I crystals and its implication for melittin's lytic and surface activities. *Biophys. J.* 37: 353–361, 1982.
- Bazzo, R., Tappin, M.J., Pastore, A., Harvey, T.S., Carver, J.A., Campbell, I.D. The structure of melittin: A 1H-NMR study in methanol. *Eur. J. Biochem.* 173:139–146, 1988.
- Vogel, H., Jahnig, F. The structure of interface in membranes. *Biophys. J.* 50:573–582, 1986.
- Brauner, J.W., Mendelsohn, R., Prendergast, F.G. Attenuated total reflectance Fourier transform infrared studies of the interaction of melittin, two fragments of melittin, and delta-hemolysin with phosphatidylcholines. *Biochemistry* 26:8151–8158, 1987.
- Vogel, H., Comparison of the conformation and orientation of alamethicin and melittin in lipid membranes. *Biochemistry* 26:4562–4572, 1987.
- Nambudripad, R., Stark, W., Opella, S.J., Makowski, L.



- Membrane-mediated assembly of filamentous bacteriophage Pf1 coat protein. *Science* 252:1305–1308, 1991.
36. Shon, J., Kim, Y., Colnago, L.A., Opella, S.J. NMR studies of the structure and dynamics of membrane-bound bacteriophage Pf1 coat protein. *Science* 252:1303–1305, 1991.
37. Nakashima, Y., Wiseman, R.L., Konigsberg, W., Marvin, D.A. Primary structure of sidechain interactions of Pf1 filamentous bacterial virus coat protein. *Nature (London)* 253:68–71, 1975.